ISSN 1063-7788, Physics of Atomic Nuclei, 2024, Vol. 87, No. 6, pp. 769–783. © Pleiades Publishing, Ltd., 2024.

ELEMENTARY PARTICLES AND FIELDS
Experiment

Measurement of Cross-Section of the ^{7}Li$(d,n)^8$Be Reactions at the Deuteron Energies from 0.4 to 2.1 MeV

S. A. Meshchaninov[1)*], A. V. Krasilnikov[1)], N. B. Rodionov[1)], Yu. A. Kashchuk[1)], S. Yu. Obudovsky[1)], A. S. Dzhurik[1)], T. M. Kormilitsyn[1)], R. N. Rodionov[1)], V. N. Amosov[1)], G. E. Nemtsev[1)], M. I. Bikchurina[2),3)], T. A. Bykov[2),3)], G. D. Verkhovod[2),3)], D. A. Kasatov[2),3)], Ya. A. Kolesnikov[2),3)], G. M. Ostreinov[2),3)], E. O. Sokolova[2),3)], and S. Yu. Taskaev[2),3),4)]**

Received July 11, 2024; revised August 30, 2024; accepted August 30, 2024

Abstract—Obtaining intense neutron fluxes are required for production of radioactive isotopes, radiation testing of promising materials, neutron diffraction, neutron capture therapy, and other applications. The interaction of deuterons with lithium is characterized by a high neutron yield, a wide variety of reactions, but the available experimental data on the reaction cross-section are scarce and contradictory, which does not allow reliably estimating the yield and spectrum of generated neutrons. In this work, effective partial cross-sections of the nuclear reactions ^{7}Li$(d,n)^8$Be with the formation of the Be nucleus in the ground and first excited states at deuteron energies from 0.4 to 2.1 MeV were measured at accelerator based neutron source VITA using the developed RBN-A1 fast neutron spectrometric radiometer. It is shown that measurements by the fast detector radiometer with two diamond spectrometric detectors provide a number of advantages over the traditionally used measuring path scintillation detector. Analysis of the high-energy part of the amplitude spectra of diamond detectors, determined by the reactions ^{12}C$(n,\alpha)^9$Be and ^{12}C$(n,\alpha)^9$Be*, allowed measuring the effective partial cross-sections of the nuclear reaction ^{7}Li$(d,n)^8$Be with the formation of the Be nucleus in the ground state and, especially, in the first excited state.

DOI: 10.1134/S1063778824700789

1. INTRODUCTION

Powerful neutron fluxes are used in many spheres of human activity, including radioactive isotopes for medicine and industry, radiation testing of modern materials and equipment, neutron diffraction analysis, and neutron capture therapy. The highest yield of neutrons per unit of current of charged particle beam at relatively low energies is given by the $T(d,n)$ reaction, and that at energies higher than 0.7 MeV is given by the Li(d,n) reaction. Interaction of deuterons with an energy below 2.2 MeV with natural lithium leads to ten nuclear reactions, five of which produce neutrons. Knowledge of the cross-section of the reactions is important for estimating the spectrum of neutrons at radiation testing of materials, for considering the possibility of using lithium as a material of the first wall and calculating the energy balance of a fusion reactor. However, the data about the cross-sections of these nuclear reactors are either rare and contradictory or absent.

In this work we present and discuss the results of measuring the cross-section of the ^{7}Li$(d,n)^8$Be and ^{7}Li$(d,n)^8$Be* reactions performed at the accelerator source of neutrons using the developed spectrometric radiometer of fast neutrons RBN-A1 with two spectrometric diamond detectors synthesized from a plasma discharge (CVD).

2. EXPERIMENTAL FACILITY

We performed the study on the accelerator source of neutrons VITA at the Budker Institute for Nuclear Physics of the Siberian Branch of the Russian Academy of Sciences (Novosibirsk, Russia) [1, 2]. Figure 1 presents the scheme of the experimental facility. In the vacuum insulated tandem accelerator *1*, a deuteron beam is formed that is directed towards the lithium target *6* through 1-mm collimator *3*. The deuteron beam has a high monochromaticity of 0.1%, a high stability of 0.1%, and the possibility of changing its energy up to 2.1 MeV. The deuteron beam

[1)]Institution Project Center ITER, State Atomic Energy Corporation Rosatom, Moscow, Russia.
[2)]Budker Institute of Nuclear Physics, Novosibirsk, Russia.
[3)]Novosibirsk State University, Novosibirsk, Russia.
[4)]Joint Institute for Nuclear Research, Dubna, Moscow oblast, Russia.
[*]E-mail: S.Meshaninov@iterrf.ru
[**]E-mail: taskaev@inp.nsk.ru

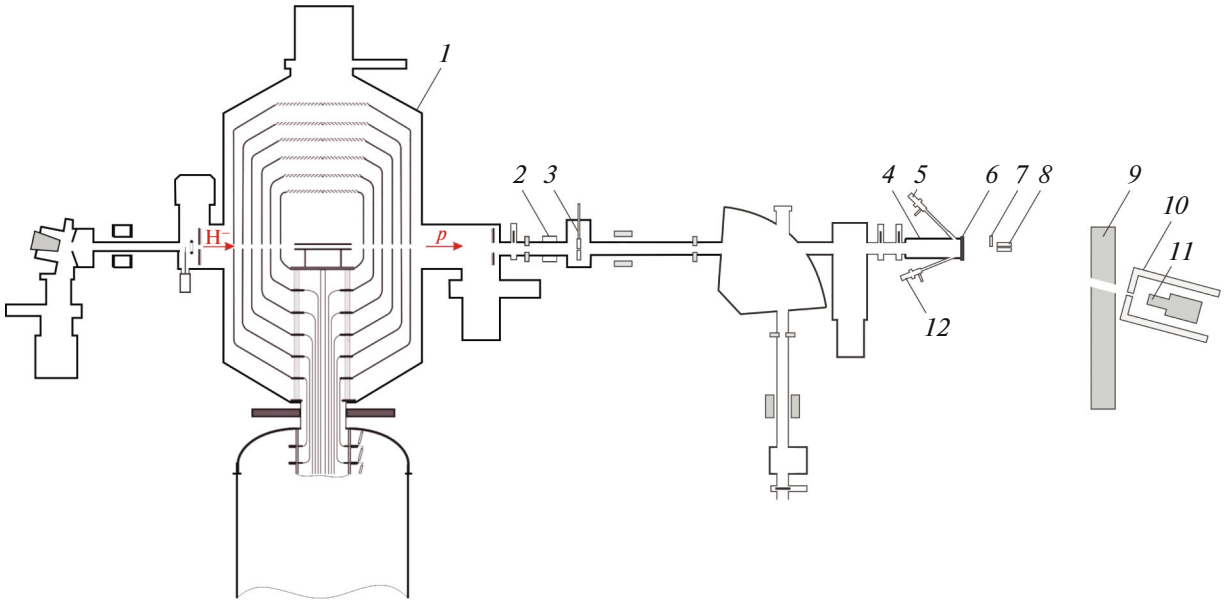

Fig. 1. Scheme of experimental facility: (*1*) vacuum insulated tandem accelerator, (*2*) contactless current sensor, (*3*) cooled collimator, (*4*) target unit, (*5*) and (*12*) α spectrometer, (*6*) lithium target, (*7*) temporarily placed lead sheet, (*8*) spectrometric radiometers of fast neutrons with diamond detector, (*9*) temporarily mounted concrete wall, (*10*) lead collimator, and (*11*) γ spectrometer.

current before the collimators is measured by the contactless current sensor NPCT (Bergoz Instrumentation, France) *2* [3] and at the lithium target by a calibrated resistance connected to the target unit electrically insulated from the facility, using the latter as a deep Faraday cup.

The lithium target is a copper disk 144 mm in diameter and 8 mm in thickness. A visually homogeneous lithium layer of crystalline density is deposited by the thermal sputtering on one side of the disk in a circle 84 mm in diameter. At the other side of the copper disk, inside a circle 122 mm in diameter, spiral-shaped channels for water colling are made; this side of the copper disk is pressed by an aluminum disk with a thickness of 16 mm. The lithium target is integrated in the target unit equipped with a gate valve and windows for observation of the target surface. For sputtering, the natural lithium produced by the Novosibirsk Plant of Chemical Concentrations is used, in which the content of lithium itself is 99.956%, and the rest admixtures form 0.044%: Na, K, Ca, Mg, Mn, Fe, Al, SiO_2, and N. The content of lithium-7 in the natural lithium varies from 92.4 [4] to 92.58% [5]. We assume that this value is equal to the average, namely, 92.5%.

The thickness of the lithium layer was measured by the proposed and implemented in situ method [6] and was 1.79 ± 0.07 μm. A detailed description of measuring the thickness of the lithium layer is given in works [7, 8].

The density of neutron flux and their energy are measured by means of two radiometers of fast neutrons RBN-A1 with spectrometric diamond detectors prepared at the private Institution Project Center ITER, State Atomic Energy Corporation Rosatom (Moscow) [9]. In one of them, designated by RBN-A1-001, the AD-1 detector is manufactured from a single-crystal CVD plate with dimensions $4.5 \times 4.5 \times 0.5$ mm^3 by the Element Six company (the contact area is 12.25 mm^2). In the other one, designated by RBN-A1-003, the B68 detector is manufactured from a single-crystal CVD film with dimensions $4.0 \times 4.0 \times 0.09$ mm^3 (the contact area is 9 mm^2) grown on a diamond substrate with the p-type conductivity and a boron concentration of $\sim$0.01% [10]. For the AD-1 and B68 detectors, the charge collection efficiency is 98 and 97%, the sensitivity to 14.7-MeV neutrons is 8.3×10^{-5} cm^2 and 4.0×10^{-6} cm^2, the energy resolution for the monoenergetic neutron line of 14.1 MeV obtained with the deuterium-tritium generator ING-07T at an angle of 90° to its axis is 134 and 214 keV, respectively. The composition of the radiometer of fast neutrons includes a detector, a charge-sensitive preamplifier, a coaxial cable with a length of 20 m, and a support unit consisting of a power supply unit and a shaping amplifier, an ADC usb-8k-v1 (AO Scientific Production Center Aspekt, Dubna, Moscow oblast), and a dedicated software.

The detectors (indicated by *8* in Fig. 1) are placed in parallel to the axis of the deuteron beam behind the lithium target at a certain distance and under different

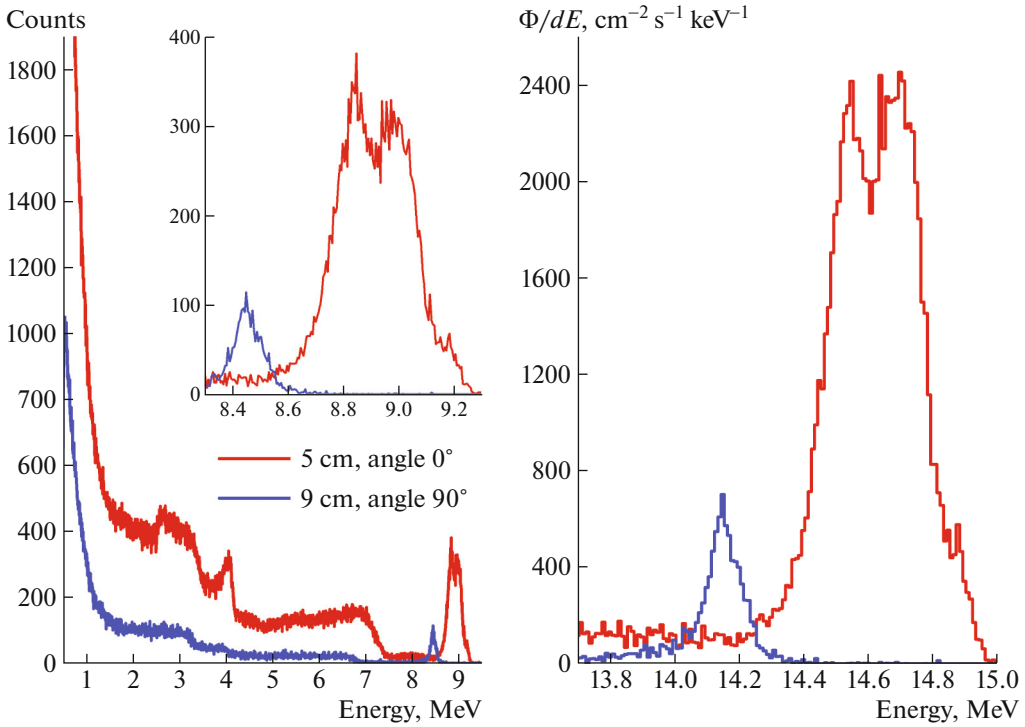

Fig. 2. Amplitude spectrum of fast neutron radiometer with diamond detector AD-1 under irradiation by neutron spectrum of deuteron-tritium generator ING-07T at angles of 0° and 90° relative to its axis and the part of the neutron spectrum recovered by it, where Φ/dE is the flux density normalized by the energy width of the channel.

angles relative to this axis; the planes of diamond detector plates are perpendicular to the registration cones. Beginning from the deuteron beam energy of 1 MeV, a 3-mm-thick lead plate is placed between the large-volume detector AD-1 and the target to suppress the low-energy γ radiation. In the case when the diamond detector was mounted perpendicularly to the deuteron beam axis, a part of copper flange with a thickness of 67 mm was mounted between the detector and the target.

Calibration of the energy scale of spectrometric radiometers was carried out using a reference spectrometric source of ^{226}Ra (pass no. 2627/5 dated September 12, 2022) with an activity of 28.47 kBq, emitting α particles with an energies of 4.75, 5.45, 5.97, and 7.65 MeV. In calibration of the spectrometric radiometers in air, we take into account experimentally determined variations in the energies of α particles at passage of 2 mm of air—the distance from the surface of the α source to the surface of the sensitive element of the detector. Additionally, to calibrate the spectrometric radiometer with the AD-1 detector, a reference spectrometric source of conversion electrons ^{137}Cs is commonly used (pass no. 1050/4 dated October 21, 2014); it has a radioactivity of 32.3 kBq and is characterized by the energy of electrons of internal conversion from the K shell of 624 keV. The dependence of the energy E on the channel number N is calculated automatically in the software Aspekt Control, assuming it a second-degree polynomial: $E\,[\text{keV}] = 64.3 + 5.91N - 1.75 \times 10^{-4} \times N^2$ for the radiometer with the AD-1 detector and $E\,[\text{keV}] = 48.8 + 6.07N - 2.45 \times 10^{-4} \times N^2$ for the radiometer with the B68 detector.

The sensitivity of the spectrometric radiometer RBN-A1-001 with the AD-1 detector was determined with a neutron deuterium–tritium generator ING-07T. The amplitude spectrum of the detector was measured at a distance of 5 cm from the generator target on its axis. The density of the neutron flux at this point was controlled by using an aluminum activation detector — a disk 31 mm in diameter and 1 mm in thickness. The flux density of $(8.59 \pm 0.29) \times 10^5$ s^{-1}cm^{-2} (3.4%) was calculated by the measured values of the induced radioactivity of ^{24}Na from the $^{27}\text{Al}(n,\alpha)^{24}\text{Na}$ reaction, and the corresponding sensitivity of the radiometer with the AD-1 detector was $(8.36 \pm 0.33) \times 10^{-5}$ cm^2 (4.0%). The average energy of the neutron flux of 14.63 MeV was determined from the amplitude spectrum of the RBN-A1-001 radiometer (Fig. 2). The right peak of the amplitude spectrum of the diamond detector was caused by the threshold reaction $^{12}\text{C}(n,\alpha_0)^9\text{Be}$ (the threshold energy is 5.7 MeV) [11–14]; therefore,

to to build the high-energy part of the neutron spectrum, we need to shift the corresponding part of the amplitude spectrum by 5.7 MeV and perform normalization by the cross-section of this reaction and the detector sensitivity.

Figure 2 also presents the neutron spectrum of the deuterium–tritium generator ING-07T at an angle of 90°, which allows determining the energy resolution (ignoring the widening of the energy line of 14.1 MeV by the generator itself) that was 0.95% for the spectrometric radiometer RBN-A1-001 with the AD-1 detector.

We similarly calibrated the sensitivity of the RBN-A1-003 with the B68 detector, as a result of which we determined the sensitivity to the neutron flux with a mean energy of 14.59 MeV that was $(4.04 \pm 0.17) \times 10^{-6}$ cm^2 (4.3%).

3. REACTIONS

Interaction between deuterons with an energy below 2.2 MeV and natural lithium nuclei leads to the following nuclear reactions [1]:

1 $^7\mathrm{Li} + d = n + {}^8\mathrm{Be} + 15.028$ MeV, $^8\mathrm{Be} \to 2\alpha + 0.094$ MeV;

2 $^7\mathrm{Li} + d = n + \alpha + \alpha + 15.121$ MeV;

3 $^7\mathrm{Li} + d = \alpha + {}^5\mathrm{He} + 14.162$ MeV, $^5\mathrm{He} \to n + \alpha + 0.957$ MeV;

4 $^6\mathrm{Li} + d = \alpha + \alpha + 22.38$ MeV;

5 $^6\mathrm{Li} + d = n + {}^7\mathrm{Be} + 3.385$ MeV;

6 $^6\mathrm{Li} + d = p + {}^7\mathrm{Li} + 5.028$ MeV;

7 $^6\mathrm{Li} + d = p + {}^7\mathrm{Li}^* + 4.550$ MeV;

8 $^6\mathrm{Li} + d = t + p + \alpha + 2.6$ MeV;

9 $^6\mathrm{Li} + d = t + {}^5\mathrm{Li} + 0.595$ MeV, $^5\mathrm{Li} \to \alpha + p + 1.965$ MeV;

10 $^6\mathrm{Li} + d = {}^3\mathrm{He} + {}^5\mathrm{He} + 0.840$ MeV, $^5\mathrm{He} \to n + \alpha + 0.957$ MeV.

The data about the cross-sections of these reactions are rare and often absent. The ENDF/B database includes only the data for the two reactions: $^6\mathrm{Li}(d,\alpha)\alpha$ and $^6\mathrm{Li}(d,p)^7\mathrm{Li}$; the TENDL database has the same reactions, but with a reference that they are borrowed from the ENDF/B database; the JENDL database has no data about these reactions. The EXFOR and IBANDL libraries provide the data from original papers, and these libraries, in addition to the data about the $^6\mathrm{Li}(d,\alpha)\alpha$ and $^6\mathrm{Li}(d,p)^7\mathrm{Li}$ reactions, include the data about the cross-sections of the $^7\mathrm{Li}(d,\alpha)^5\mathrm{He}$ ($^5\mathrm{He} \to \alpha + n$) and $^6\mathrm{Li}(d,p)^7\mathrm{Li}^*$ reactions. Thus, among 10 nuclear reactions of interaction between deuteron and natural lithium, in five of which neutrons are emitted, there are data about the cross-sections of only four nuclear reactions, in one of which neutrons are emitted. In a recent work [8], Taskaev et al. presented the results of measuring the cross-sections of these four reactions, as well as of the $^7\mathrm{Li}(d,n)2\alpha$ reaction providing the largest yield of neutrons. In the current work, the object of our study is measuring the cross-section of the $^7\mathrm{Li}(d,n)^8\mathrm{Be}$ reaction characterized by the highest energy of generated neutrons. The remaining two reactions of neutron generation, $^6\mathrm{Li}(d,n)^7\mathrm{Be}$ and $^6\mathrm{Li}(d,{}^3\mathrm{He})^5\mathrm{He}$ ($^5\mathrm{He} \to \alpha + n$), are complicated for measurements because of a low energy of reaction products, but, due to a low content of ^{6}Li isotope in the natural lithium, they can make a small contribution to the total yield of neutrons. Thus, in this work we add the data about the $^7\mathrm{Li}(d,n)^8\mathrm{Be}$ reactions, which allows more reliably estimating the yield and energy spectrum of neutrons in the high-energy part of the spectrum.

4. MEASUREMENT OF CROSS-SECTION OF REACTION

The cross-section of the $^7\mathrm{Li}(d,n)^8\mathrm{Be}$ reaction is measured as follows. We irradiated a thin layer of the lithium target and record the amplitude spectra of the diamond detectors of the radiometer of fast neutrons in a certain solid angle. We determine the differential cross-section of the reaction in the laboratory coordinates $d\sigma/d\Omega$ by the formula

$$\frac{d\sigma}{d\Omega} = \frac{e\Phi}{nl_{\mathrm{Li}} I_d \Omega_{\mathrm{lab}}} \frac{1}{(1 - k_{\mathrm{abs}})},$$

where e is the electron charge, n is the density of ^{7}Li nuclei equal to $(4.251 \pm 0.004) \times 10^{22}$ cm^{-3}, l_{Li} is the thickness of the lithium layer equal to $(1.79 \pm 0.07) \times 10^{-4}$ cm, I_d is the current of deuterons, k_{abs} is the coefficient of attenuation of the neutron flux at passage of the monoenergetic neutron flux through the structural materials, Ω_{lab} is the solid angle (Table 1, [15]), Φ is the neutron flux density determined by the formula

$$\Phi = \frac{Y}{Tk\,(\sigma_{^{12}\mathrm{C}})},$$

where $k\,(\sigma_{^{12}\mathrm{C}})$ is the sensitivity of the radiometer detector depending on the cross-section of the $^{12}\mathrm{C}(n,\alpha_0)^9\mathrm{Be}$ reaction, Y is the experimentally determined number of useful events in the analysis region, and T is the measurement time.

To determine the coefficient of attenuation of the neutron flux with a mean energy of 14.6 MeV, we performed additional measurements of the neutron flux density under the deuterium–tritium generator ING-07T. Between the generator target and the detector we placed materials corresponding to the structure of the neutron source VITA at different positions of

Table 1. Values of normalizing coefficients

Mean energy of deuterons in reaction, keV	RBN-A1-001 with detector AD-1			RBN-A3-001 with detector B68		
	solid angle, $\times 10^{-2}$ sr	coefficient of monoenergetic neutron flux attenuation with formation of Be		solid angle, $\times 10^{-2}$ sr	coefficient of monoenergetic neutron flux attenuation with formation of Be	
		in the ground state	in the first excited state		in the ground state	in the first excited state
333	1.060	0.234		5.327	0.291	
441	2.118	0.258		1.978	0.274	
760	1.266	0.260	0.278	5.327	0.289	0.303
864	1.940	0.648	0.676	5.327	0.289	0.302
962	3.660	0.280	0.296	3.909	0.241	0.253
1064	3.660	0.280	0.296	3.909	0.241	0.252
1170	3.660	0.279	0.296	3.909	0.240	0.252
1270	3.660	0.279	0.295	3.909	0.240	0.251
1372	3.660	0.279	0.295	3.909	0.239	0.250
1473	3.660	0.278	0.295	3.909	0.239	0.250
1573	3.660	0.278	0.294	3.909	0.238	0.249
1674	3.660	0.278	0.294	3.909	0.238	0.249
1776	3.660	0.278	0.293	3.909	0.238	0.248
1877	3.660	0.278	0.293	3.909	0.238	0.248
1977	3.660	0.277	0.293	3.909	0.237	0.247
2078	3.660	0.277	0.293	3.909	0.237	

the detector, after which we measured the amplitude spectrum of the diamond detector AD-1 included in the RBN-A1-001 radiometer. Because it is impossible to experimentally determine the coefficient of attenuation of the monoenergetic neutron flux of different energy, the coefficients of attenuation at different energy of neutron flux are determined by normalizing the coefficient of attenuation of neutron flux with a mean energy of 14.55–14.59 MeV by the relative variation in the values of the total cross-section of interaction between neutrons and the corresponding materials. The values of the total cross-section of interaction between neutrons and the corresponding materials was determined according to their isotope composition (the isotope composition of the natural copper: ^{63}Cu (69.1%) and ^{65}Cu (30.9%), the composition of duralumin: ^{27}Al (90–95%), and the composition of lead: ^{206}Pb (46.2%) and ^{208}Pb (52.4%)). We calculated the coefficient of attenuation of the monoenergetic neutron flux at passage though the structural materials with insignificant variations in the thickness also by normalizing by the relative variation in the neutron flux density obtained from the exponential law of attenuation of the neutron flux density [16]. Table 1 presents the calculation results.

5. ^{7}Li$(d,n)^{8}$Be REACTION

The ^{7}Li$(d,n)^{8}$Be reaction leads to generation of a neutron and a beryllium nucleus, and the beryllium nucleus can occur in either the ground or excited state: $\Gamma_{^{8}\mathrm{Be}} \sim 10$ eV, $E_{^{8}\mathrm{Be}^{*}} \approx 2.9$ MeV at $\Gamma_{^{8}\mathrm{Be}^{*}} \sim 0.8$ MeV. Figure 2 presents a typical amplitude spectrum of the detector placed at an angle of 90° to the axis of the deuterium–tritium neutron generator under a monoenergetic neutron flux with an energy of 14.1 MeV, and Fig. 3a shows the amplitude spectrum under the target of the VITA facility.

We reconstructed the high-energy part of the neutron spectra by normalizing the spectral response of the diamond detector to the cross-section of the

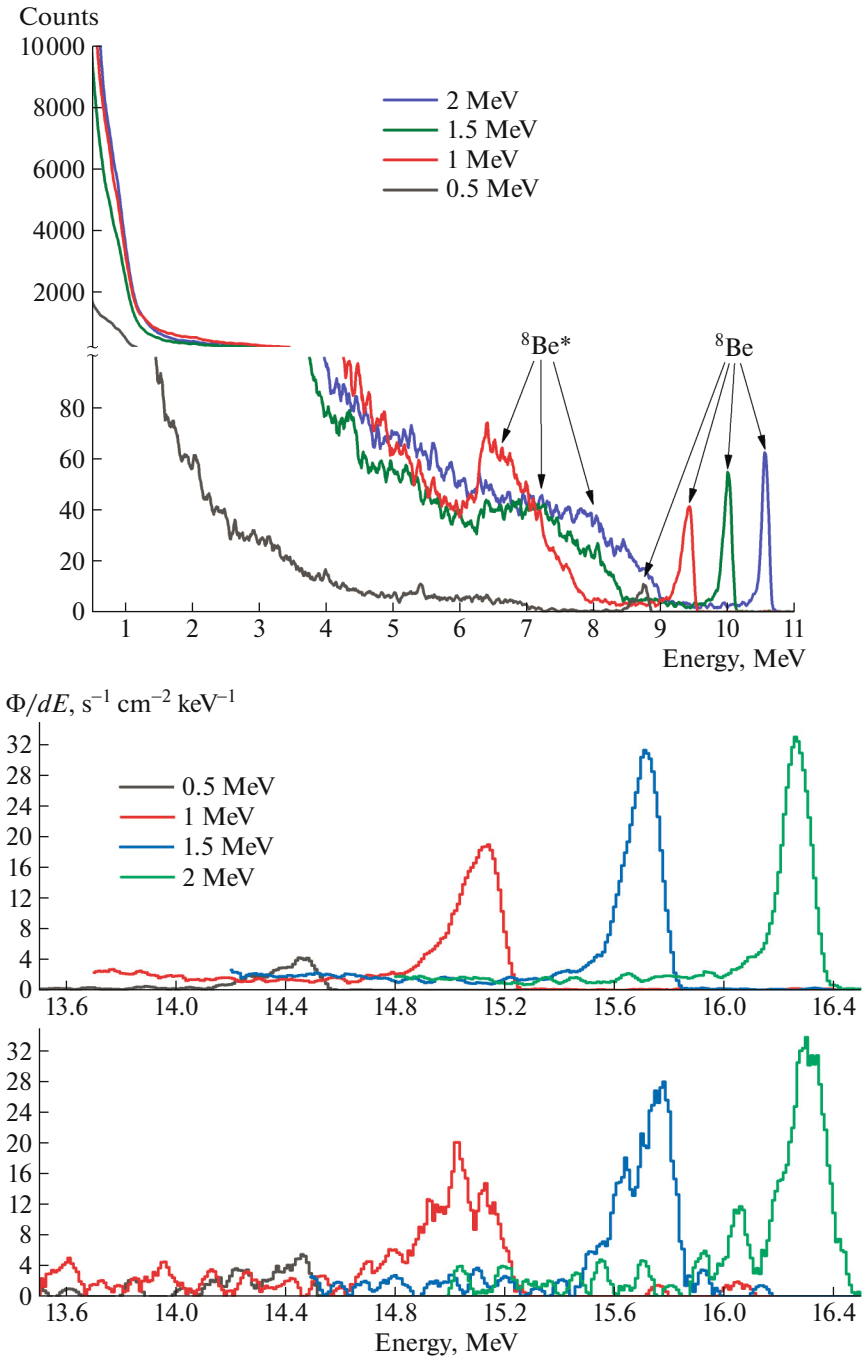

Fig. 3. (*a*) Amplitude spectra of fast neutron radiometer with large-size diamond detector AD-1 under irradiation of the VITA facility with different values of incident deuteron energy. (*b*) Spectra of neutrons obtained from these amplitude spectra (top) and similar amplitude spectra of diamond detectors of different sensitivity (AD-1 is top and B68 is bottom), where Φ/dE is the flux density normalized by the energy width of the channel.

$^{12}C(n,\alpha_0)^9Be$ reaction taking into account the energy threshold of 5.7 MeV. We used the cross-section of the reaction from work [13], because it was determined with a lower uncertainty with a similar quality of materials. The right peak of the neutron spectrum was caused by neutrons produced in the $^7Li(d,n)^8Be$ reaction with formation of ^8Be in the ground state. In the energy range of 6–8 MeV of the amplitude spectra of the diamond detector, we see an additional bump caused by neutrons from the same reaction, but with formation of $^8Be^*$ in the first excited state, which will be considered below. The high-energy peak was approximated by the Gaussian distribution with fixation of its center, full width at half-maximum,

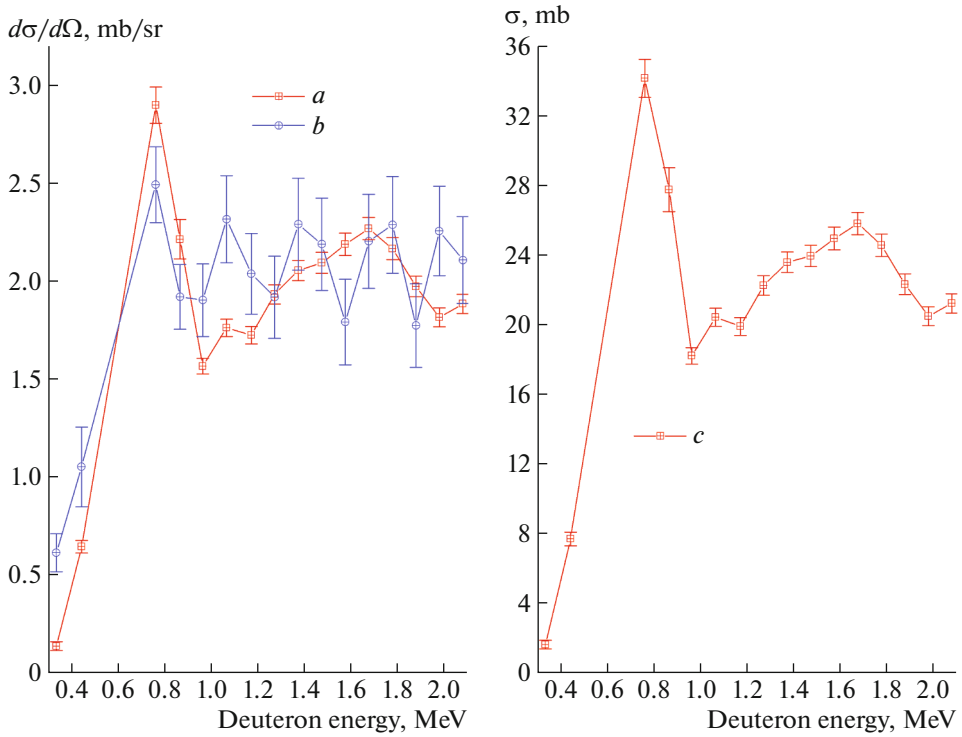

Fig. 4. (a, b) Differential and (c) effective partial cross-sections of the $^{7}\mathrm{Li}(d, n)^{8}\mathrm{Be}$ reaction with formation of $^{8}\mathrm{Be}$ in the ground state determined by the amplitude spectra of two different diamond detectors with indication of statistical error.

and area (Tables 2 and 3). In addition to that, in the amplitude spectra we see two noticeable steps: in the regions of 1.5–4 MeV and 1–1.5 MeV, which correspond to the neutron groups with a lower energy, but we do not perform their analysis in this work.

We compared the experimentally data of the mean energy of neutron flux with the calculation results of the kinematics of the $^{7}\mathrm{Li} + d = n + {}^{8}\mathrm{Be} + 15.028$ MeV reaction [17] for both the diamond detectors. In addition to well agreement with the calculated values, for both spectrometric radiometers we see a deviation that is small but increasing with the deuteron energy, which can be caused both by calibration error and by physical parameters of the VITA facility (for instance, by variation in the focusing of the deuteron beam as its energy increases, which leads to actual change in the distance from the neutron source to the detector with a change in the angle). The width of the resonance with formation of the beryllium nucleus in the ground state is quite small and is approximately 10 eV [16]; therefore, we can state that the width of the experimentally obtained peak is determined by the energy resolution of the detector itself, by the loss of deuteron energy in the target, and by spreading the neutron spectrum at passage through the structural materials from the target to the detector, which can be ignored. As a result of estimation at the energy range of incident deuterons from 1 to 2 MeV, the full width at half-maximum of the RBN-A1-001 detector decreases from 1.2 to 0.75%.

The obtained data allow determining the differential cross-section of the $^{7}\mathrm{Li}(d, n)^{8}\mathrm{Be}$ reaction with formation of $^{8}\mathrm{Be}$ in the ground state. Because the differential cross-sections measured by both the detectors do not differ from each other within the range of uncertainties, the reaction can be assumed isotropic (Fig. 4, Tables 4 and 5).

The uncertainty in measuring the cross-section is determined by the uncertainty in the measurement of lithium thickness (4%), the uncertainty of determining the sensitivity of detectors (no larger than 4.3%), the uncertainty of detector mounting (no more than 2%), the uncertainty of determining the coefficient of attenuation of the monoenergetic neutron flux at passage through structural materials (4%), the uncertainty of determining the density of atomic nuclei of lithium (1%), and the standard error (1–1.5%); in total, it is no more than 7.6%. The uncertainty of determining the angle is $\pm 1^{\circ}$. The uncertainty of determining the cross-section of the $^{12}\mathrm{C}(n, \alpha_0)^{9}\mathrm{Be}(\delta_{c12})$ reaction and the statistical error $(d\sigma_i/d\Omega_i)$ are given in Tables 4 and 5.

The main works in which the absolute measurements of the effective partial cross-section of $^{7}\mathrm{Li}(d, n)^{8}\mathrm{Be}$ with formation of $^{8}\mathrm{Be}$ were performed

Table 2. Neutron flux density of reaction ^{7}Li$(d, n)^{8}$Be measured by RBN-A1-001 with AD-1 detector

Energy of incident deuterons, MeV	Mean loss of deuteron energy in target, keV	Angle from axis, deg	Distance, cm	Mean current of beam, μA	Lifetime, s	Position of neutron peak, MeV	FWHM of neutron peak, keV	Density of neutron flux, $s^{-1}cm^{-2}$
0.4	72	9	9.7	1.745	5399.58	14.36	153	92
0.5	63	29	6.85	1.823	5398.12	14.52	218	877
0.8	47	30	8.87	1.692	5396.32	14.63	207	2182
0.9	43	90	7.16	1.815	5396.02	13.93	130	1303
1	41	20	5.2	1.915	5388.01	15.24	197	3754
1.1	38	20	5.2	1.741	5387.57	15.37	158	3840
1.2	37	20	5.2	1.825	5390.15	15.50	171	3944
1.3	34	20	5.2	1.815	5390.88	15.63	153	4397
1.4	32	20	5.2	1.872	5390.91	15.76	154	4822
1.5	31	20	5.2	1.859	5390.45	15.88	146	4884
1.6	29	20	5.2	1.810	5389.61	16.00	140	4969
1.7	28	20	5.2	1.903	5387.53	16.13	128	5418
1.8	27	20	5.2	1.853	5385.4	16.25	122	5035
1.9	26	20	5.2	1.879	5385.18	16.37	127	4654
2	25	20	5.2	1.905	5385.08	16.48	119	4347
2.1	24	20	5.2	1.827	5383.76	16.60	126	4327

Table 3. Neutron flux density of reaction ^{7}Li$(d, n)^{8}$Be measured by RBN-A1-003 with B68 detector (the lifetime is 5399.3 s)

Deuteron energy, MeV	Angle from axis, deg	Distance, cm	Mean current of beam, μA	Position of neutron peak, MeV	FWHM of neutron peak, keV	Density of neutron flux, $s^{-1}cm^{-2}$
0.4	38	4.3	1.745	14.31	153	1920
0.5	32	7.09	1.823	14.36	321	1308
0.8	38	4.3	1.692	14.58	250	7583
0.9	38	4.3	1.815	14.70	232	6267
1	13	5.03	1.915	15.02	325	5134
1.1	13	5.03	1.741	15.24	216	5683
1.2	13	5.03	1.825	15.35	242	5248
1.3	13	5.03	1.815	15.58	217	4913
1.4	13	5.03	1.872	15.61	225	6060
1.5	13	5.03	1.859	15.73	217	5749
1.6	13	5.03	1.810	15.87	170	4586
1.7	13	5.03	1.903	15.96	184	5932
1.8	13	5.03	1.853	16.05	200	5996
1.9	13	5.03	1.879	16.15	212	4714
2	13	5.03	1.905	16.30	170	6089
2.1	13	5.03	1.827	16.41	189	5455

are works [18–21], included in the EXFOR database [22]. Only two works [20, 21] use measurement of the angular energy distribution of the neutron flux density to determine the effective partial cross-section of this reaction. The relative angular energy distributions of the neutron flux density weakly correlate with

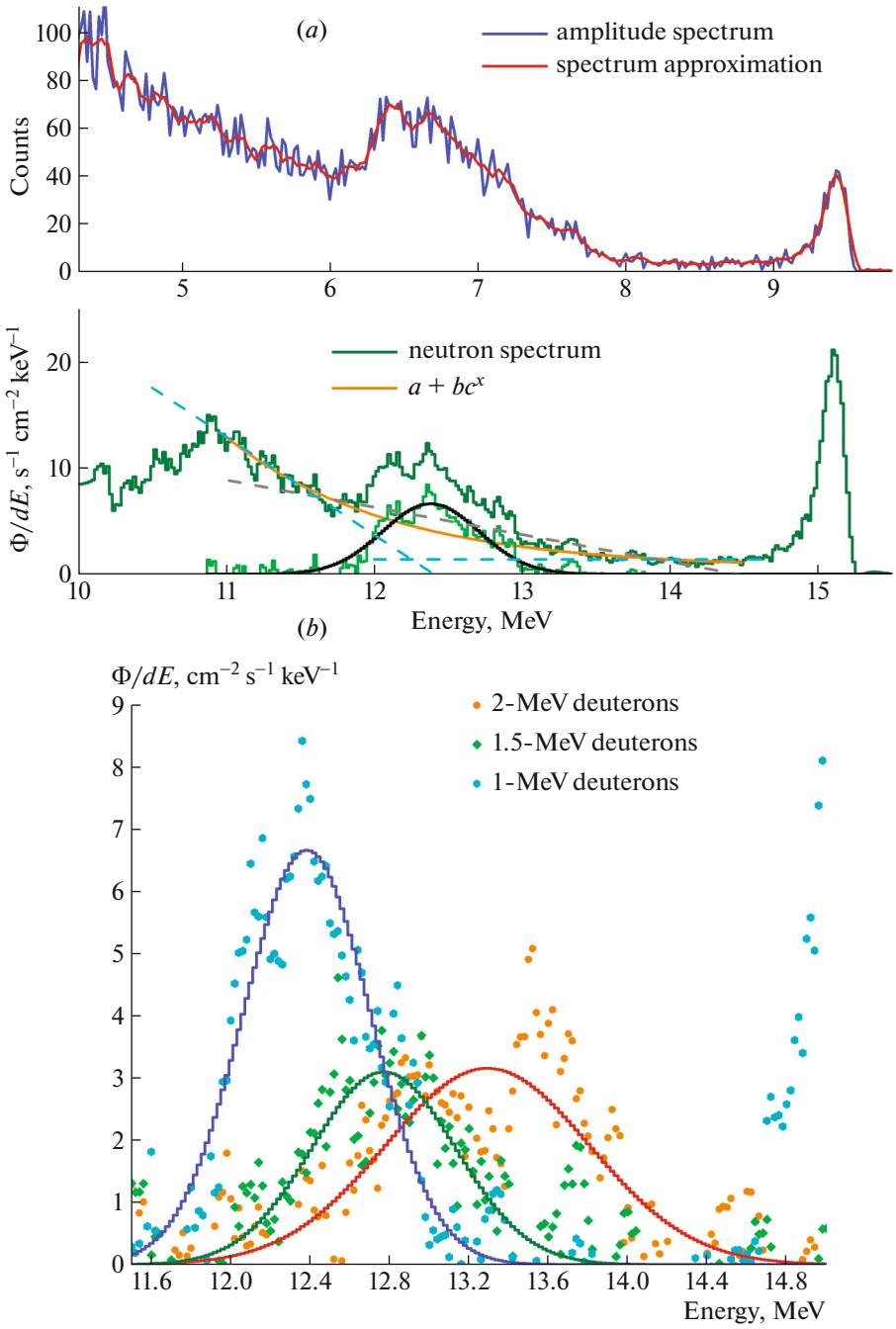

Fig. 5. (*a*) At the top, the amplitude spectrum of large-volume diamond detector (AD-1) under irradiation of the VITA facility at 1 MeV of incident deuteron energy (blue color), its approximation by the function of the diamond detector response (red) and, at the bottom, the recovered neutron spectrum (green), where Φ/dE is the flux density normalized by the energy width of the channel. At the bottom graph, we also present the approximating function of background $y = a + bc^x$ (orange color), limiting approximating functions of background from two straight lines (light-blue dashed curve) and one straight line (gray dashed curve), an isolated peak corresponding to the nuclear reaction ^{7}Li$(d, n)^8$Be* (light-green color), and its approximation by the Gaussian distribution (black). (*b*) Isolated neutron spectra obtained by the RBN-A1-001 corresponding to the first excited level of the ^{8}Be* nucleus with their approximation by the Gaussian distribution for energies of incident deuterons of 1, 1.5, and 2 MeV.

each other, and the dependences revealed by different authors are nonequal and can be caused by the attenuation of the neutron flux at passage through the structural materials that characteristic for their facilities. By the differential cross-sections, the best coincidence of the results obtained in this work at

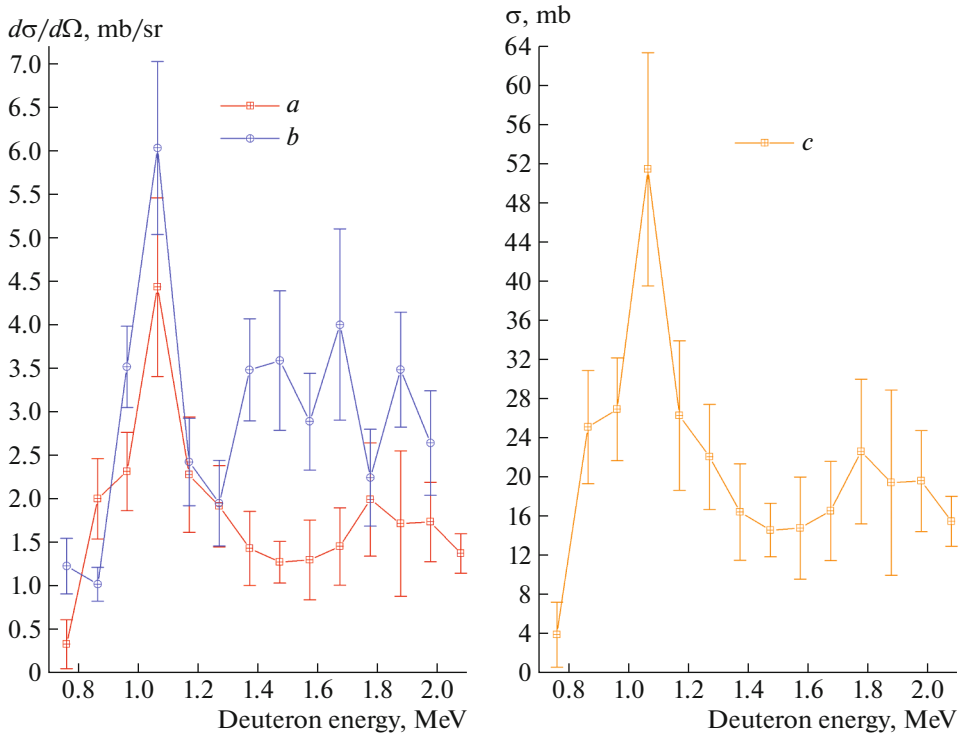

Fig. 6. (a, b) Differential and (c) partial cross-sections of the $^{7}\mathrm{Li}(d,n)^{8}\mathrm{Be}^{*}$ reaction with formation of $^{8}\mathrm{Be}^{*}$ in the first excited state determined by measurements of response spectra of two diamond detectors of different sensitivity with indication of the root of sum of squares of the statistical error and the error of uncertainty in the background function.

deuteron energies of 0.4–0.5 MeV is observed with the results of Dai Nengxiong et al. [19] measured at an angle of 90°, the results at deuteron energies of 0.8–1.5 MeV best agree with the results by Bochkarev et al. [18] measured at an angle of 0°, and the results at deuteron energies of 1.5–2.1 MeV best agree with the results by Osetinskii et al. [21] measured at an angle of 120°. The effective partial cross-section of the $^{7}\mathrm{Li}(d,n)^{8}\mathrm{Be}$ reaction with formation of $^{8}\mathrm{Be}$ in the ground state is below the values measured in works [20, 21]. Because the angles at which both detectors were placed relative to the beam of incident deuterons are not so different from each other, the assumption about the isotropic character of this reaction can be false. In several works of other authors, the measurement results of the relative angular energy distributions of the neutron flux density corresponding to the nuclear reaction $^{7}\mathrm{Li}(d,n)^{8}\mathrm{Be}$ with formation $^{8}\mathrm{Be}$ in the ground state can also be assumed isotropic within the measurement uncertainty [20, 21, 23–25].

6. $^{7}\mathrm{Li}(d,n)^{8}\mathrm{Be}^{*}$ REACTION

The $^{7}\mathrm{Li}(d,n)^{8}\mathrm{Be}^{*}$ reaction leads to formation of a neutron and a beryllium nucleus in the first excited state $E_{^{8}\mathrm{Be}^{*}} \approx 2.9$ MeV at $\Gamma_{^{8}\mathrm{Be}^{*}} \sim 0.8$ MeV. Reconstruction of the high-energy part of the neutron spectra caused by this channel of the nuclear reaction is sophisticated not only by superposition upon the neutron group with a wide energy distribution from the $^{7}\mathrm{Li}(d,n\alpha)^{4}\mathrm{He}$ reaction, but also by superposition upon the amplitude spectra caused by the higher-energy part of the neutron spectrum, including the above considered reaction with formation of a $^{8}\mathrm{Be}$ nucleus in the ground state (the channels of the $^{12}\mathrm{C}(n,3\alpha)$ reaction by diamond). The best decision would be to use the experimental spectral responses under monoenergetic neutron beams obtained, e.g., in work [13], but, unfortunately, they are not given in the complete form; therefore, we apply a traditional approach to reconstruction of the neutron spectra on the basis of the response function of the diamond detector obtained with the Geant4 software. The response function of the diamond detector calculated with the Geant4 software [26] associates the group spectrum of the neutrons incident to the detector and the amplitude spectrum of the detector (the mean number of counts in the channels of a conventional ADC, where the number of the channel corresponds to the value of the energy spent by the reaction products). In addition to a high uncertainty, a disadvantage of this approach is as follows: when recovering the neutron spectrum, we observe a rather strong

Table 4. Differential cross-section of the ^{7}Li$(d,n)^8$Be reaction with formation of ^{8}Be in the ground state

E, keV	θ_1, deg	$d\sigma_1/d\Omega_1$, mb/sr	$\Delta d\sigma_1/d\Omega_1$, mb/sr	θ_2, deg	$d\sigma_2/d\Omega_2$, mb/sr	$\Delta d\sigma_2/d\Omega_2$, mb/sr	δ_{c12}, %
333	9	0.12	0.02	38	0.40	0.06	6.3
441	29	0.57	0.03	32	0.67	0.13	6.4
760	30	3.28	0.10	38	1.86	0.14	6.4
864	90	1.73	0.08	38	1.53	0.13	6.6
962	20	1.74	0.04	13	1.64	0.16	6.4
1064	20	1.96	0.05	13	1.95	0.19	6.6
1170	20	1.87	0.05	13	1.69	0.17	6.8
1270	20	1.96	0.05	13	1.51	0.16	6.8
1372	20	2.06	0.05	13	1.79	0.18	6.8
1473	20	2.17	0.06	13	1.73	0.19	7.0
1573	20	2.37	0.06	13	1.49	0.18	7.0
1674	20	2.55	0.06	13	1.90	0.21	7.0
1776	20	2.50	0.06	13	2.01	0.22	7.0
1877	20	2.38	0.06	13	1.62	0.19	6.8
1977	20	2.35	0.06	13	2.15	0.22	6.8
2078	20	2.27	0.06	13	2.01	0.21	6.9

deviation of the calculation results and the experimental data with appearance of additional extremums that are unprovoked in the region of the anticipated neutron peak from the nuclear reaction ^{7}Li$(d,n)^8$Be* [27].

Table 5. Effective partial cross-section of the ^{7}Li$(d,n)^8$Be reaction with formation of ^{8}Be in the ground state

E, keV	ΔE, keV	σ_1, mb	δ_{st}, %	δ_{c12}, %
333	72	1.64	15.7	6.3
441	63	7.71	5.1	6.4
760	47	34.16	3.2	6.4
864	43	27.77	4.6	6.6
962	41	18.23	2.6	6.4
1064	38	20.44	2.5	6.6
1170	37	19.91	2.6	6.8
1270	34	22.27	2.5	6.8
1372	32	23.60	2.5	6.8
1473	31	23.96	2.6	7.0
1573	29	24.97	2.6	7.0
1674	28	25.83	2.5	7.0
1776	27	24.57	2.6	7.0
1877	26	22.34	2.6	6.8
1977	25	20.51	2.6	6.8
2078	24	21.24	2.6	6.9

Figure 5 shows the characteristic amplitude spectrum of the diamond detector under irradiation of the VITA facility at 1 MeV of incident deuteron energy with the result of neutron spectra reconstruction in the energy range corresponding to the nuclear reaction with formation of the beryllium first excited state.

By approximating the amplitude spectra at different incident deuteron energies with the response function of the diamond detector, we obtained the energy spectra of neutrons (Fig. 5*a*, bottom), where in the vicinity of the anticipated peak we highlighted the background in the form of function $\Phi(E) = a + bc^E$, corresponding to a wide energy neutron distribution from the ^{7}Li$(d,n\alpha)^4$He reaction and the scattered component of the neutron group corresponding to the formation of a ^{8}Be nucleus in the ground state; the difference between them allowed isolating the neutron peak caused by the neutron group corresponding to generation of a ^{8}Be* nucleus in the first excited state (Fig. 5*b*). To estimate the uncertainty in the background function, we considered the two additional functions corresponding to the limiting values of the peak integral corresponding to the nuclear reaction ^{7}Li$(d,n)^8$Be* (Fig. 5*a*, bottom). It is important to

Table 6. Neutron flux density of the ^{7}Li$(d,n)^8$Be* reaction measured by the RBN-A1-001 (the mean loss of deuteron energy in target, the angle from the axis, the distance to the target, the mean current of beam, and the lifetime are given in the corresponding columns of Tables 3 and 4)

Energy of incident deuteron, MeV	RBN-A1-001 with AD-1 detector			RBN-A1-003 with B68 detector		
	neutron peak position, MeV	FWHM of neutron peak, keV	neutron flux density, $s^{-1}cm^{-2}$	neutron peak position, MeV	FWHM of neutron peak, keV	neutron flux density, $s^{-1}cm^{-2}$
0.8	12.26	0.33	243	12.04	1.21	3662
0.9	11.10	0.77	1084	12.10	0.53	3263
1	12.38	0.77	5418	12.50	1.21	9342
1.1	12.38	0.92	9441	12.51	1.10	14 573
1.2	12.52	0.93	5084	12.65	0.84	6144
1.3	12.61	0.88	4255	12.45	1.15	4920
1.4	12.71	0.87	3281	12.85	1.16	9072
1.5	12.76	0.90	2900	13.24	1.56	9292
1.6	12.95	0.95	2880	13.14	1.36	7282
1.7	12.92	1.16	3391	13.11	1.66	10 618
1.8	13.07	1.32	4533	13.53	1.04	5798
1.9	13.23	1.38	3960	13.49	1.22	9145
2	13.30	1.21	4061	13.60	0.99	7034
2.1	13.37	1.09	3083			

note that the peak in the vicinity of 11 MeV is caused not by physical phenomena, but by imperfect approximation of the response function of the diamond detector. The uncertainty in the background function predominates and is determined as the standard deviation of the peak integral corresponding to the nuclear reaction ^{7}Li$(d,n)^8$Be* obtained using three different functions.

Because stability and a high value of the energy resolution of the spectrometer at variation in the deuteron beam energy is confirmed by the neutron peak corresponding to the nuclear reaction with formation of a ^{8}Be nucleus in the ground state, it appears to be possible to determine the mean excitation energy of the ^{8}Be* nucleus and its average width. By the results obtained with the spectrometric radiometer RBN-A1-001, the energy of the first excited state of the ^{8}Be* nucleus was 2.88 ± 0.13 MeV, and its width was 0.96 ± 0.27 MeV. We obtained well agreement in comparison of the experimentally obtained data of the mean energy of neutron flux with the results of the kinematic calculation of the $^7\mathrm{Li} + d = n + {}^8\mathrm{Be} + 15.028$ MeV [17] reaction taking into account the energy for excitation of the ^{8}Be* nucleus of 2.88 MeV for both diamond detectors (Table 6).

The obtained data allow determining the differential cross-section of the ^{7}Li$(d,n)^8$Be* reaction with formation of ^{8}Be* in the first excited state. When the incident deuteron beam energy is 400 and 500 keV, we detected no neutron peak corresponding to formation of ^{8}Be*. The differential cross-sections obtained by the small-size detector have a larger spread and a low confidence because of the number of counts insufficient for reconstruction of neutron spectra, but, nevertheless, they well agree with the measurement results obtained by the large-size detector AD-1 especially in the energy range 0.7–1.1 MeV. We determine the effective partial cross-section of the reaction assuming the reaction isotropic (Fig. 6, Table 7).

The uncertainty of the cross-section measurement is determined by the uncertainty of determining the thickness of lithium (4%), the uncertainty of determining the detector sensitivity (no more than 4.3%), the uncertainty of detector placement (no more than 2%), the uncertainty of determining the coefficient of attenuation of the monoenergetic neutron flux at passage through the structural materials (4%), the uncertainty of determining the density of Li nuclei (1%),

Table 7. Differential and integral cross-section of the ^{7}Li$(d,n)^{8}$Be* reaction with formation of ^{8}Be* in the first excited state

E, keV	ΔE, keV	θ_1, deg	$d\sigma_1/d\Omega_1$, mb/sr	$\Delta\sigma_1/d\Omega_1$, mb/sr	σ, mb	$\Delta\sigma$, mb
760	47	30	0.33	0.28	3.91	3.3
864	43	90	2.00	0.46	25.1	5.8
962	41	20	2.31	0.45	26.9	5.2
1064	38	20	4.43	1.03	51.8	11.9
1170	37	20	2.28	0.66	26.3	7.6
1270	34	20	1.91	0.47	22.1	5.4
1372	32	20	1.43	0.43	16.4	4.9
1473	31	20	1.27	0.24	14.6	2.7
1573	29	20	1.30	0.46	14.8	5.2
1674	28	20	1.45	0.44	16.5	5.1
1776	27	20	1.99	0.65	22.6	7.4
1877	26	20	1.71	0.84	19.4	9.5
1977	25	20	1.73	0.46	19.6	5.2
2078	24	20	1.37	0.23	15.5	2.5

the sum of uncertainty of determining the cross-section of nuclear neutron reactions by carbon from the ENDF/B-VIII.0 database used in the Geant4 software, the approximation error (no more than 20 + 5%), and the standard deviation (1–1.5%); in total, it is no more than 26.1%. The uncertainty of determining the angle is ±1°. The square root of the sum of squares of the statistical error and the uncertainty of background function ($\Delta d\sigma_i/d\Omega_i, \Delta\sigma$) is given in Table 7.

The main works in which the absolute measurements of the effective partial cross-section of ^{7}Li$(d,n)^{8}$Be with formation of ^{8}Be* were performed are papers [18–21], included in the EXFOR database [22]. Only two works [20, 21] use measurement of the angular energy distribution of the neutron flux density to determine the effective partial cross-section of this reaction. The angular distributions of the cross section of the reaction, as in the case of formation of ^{8}Be nucleus in the ground state weakly correlate to each other, and the dependences revealed by different authors are nonequal and can be caused by attenuation of the neutron flux at passage through the structural materials characteristic of their facilities, by the energy resolution of detectors they used, and by the algorithm for isolating the neutron peak from the nuclear reaction ^{7}Li$(d,n)^{8}$Be* against the background of other components of the amplitude spectra. The values of both differential and effective partial cross-sections obtained in the current work lie significantly below the values measured by the other authors, which is caused by using a spectrometric equipment of higher quality and better subsequent processing of the obtained data. The position of the resonance maximum of this nuclear reaction is higher than that of all previous researchers, which indicates the fact that, in contrast to them, the analyzed peak on the amplitude spectra of the detector does not contain counts caused by contribution of the nuclear reactions ^{7}Li$(d,n)^{8}$Be with a resonance maximum below 0.8 MeV and ^{7}Li$(d,n\alpha)^{4}$He* with a mixture of resonance maximums below 1.1 MeV [8].

An assumption about the isotropy of this reaction can be erroneous, but the results of measuring the angular distribution of the partial cross-section of the ^{7}Li$(d,n)^{8}$Be* reaction with formation of ^{8}Be* in the first excited state by other authors can be assume isotropic within the measurement uncertainty [20, 21, 24, 28].

Just one work [28] speaks about observation of the nuclear reaction ^{7}Li$(d,n)^{8}$Be** with formation of the second excited state ^{8}Be** with an energy of 11.7 MeV, but this seems to be somewhat pretending, because, in addition to a wide neutron distribution of ^{7}Li$(d,n\alpha)^{4}$He, exactly this energy range must contain a peak of the ^{6}Li$(d,n)^{7}$Be reaction, to say nothing

about the background gamma radiation and contribution of higher-energy neutron nuclear reactions. On the basis of the above discussed, we can state that in the considered energy range we determined all effective partial cross-sections of the nuclear reaction ^{7}Li$(d,n)^{8}$Be.

7. CONCLUSIONS

We measured the effective partial cross-sections of the nuclear reactions ^{7}Li$(d,n)^{8}$Be with formation of a Be nucleus in the ground and first excited states. We measured the energy and the width of the first excited level of the ^{8}Be* nucleus. We showed the advantages and possibilities of applying the spectrometric diamond detectors as a component of the radiometer of fast neutrons RBN-A1 (Institution Project Center ITER, State Atomic Energy Corporation Rosatom, Troitsk, Moscow, Russia [9]).

FUNDING

The study is supported by the Russian Science Foundation, project no. 19-72-30005, https://rscf.ru/project/19-72-30005/.

CONFLICT OF INTEREST

The authors of this work declare that they have no conflicts of interest.

REFERENCES

1. S. Yu. Taskaev, *VITA Neutron Accelerator Source* (Fizmatlit, Moscow, 2024).
2. S. Taskaev, E. Berendeev, M. Bikchurina, T. Bykov, D. Kasatov, I. Kolesnikov, A. Koshkarev, A. Makarov, G. Ostreinov, V. Porosev, S. Savinov, I. Shchudlo, E. Sokolova, I. Sorokin, T. Sycheva, and G. Verkhovod, Biology **10**, 350 (2021). https://doi.org/10.3390/biology10050350
3. NPCT: Non-destructive DC beam current measurement. https://www.bergoz.com/products/npct/.
4. P. A. de Groot, *Handbook of Stable Isotope Analytical Techniques* (Elsevier, 2009), Vol. 2.
5. K. Lieberman, G. J. Alexander, and J. A. Sechzer, Experientia **42**, 985 (1986). https://doi.org/10.1007/bf01940701
6. D. Kasatov, I. A. Kolesnikov, A. Koshkarev, A. Makarov, E. Sokolova, I. Shchudlo, and S. Taskaev, J. Instrum. **15**, P10006 (2020). https://doi.org/10.1088/1748-0221/15/10/p10006
7. S. Taskaev, M. Bikchurina, T. Bykov, D. Kasatov, I. Kolesnikov, A. Makarov, G. Ostreinov, S. Savinov, and E. Sokolova, Nucl. Instrum. Methods Phys. Res., Sect. B **525**, 55 (2022). https://doi.org/10.1016/j.nimb.2022.06.010
8. S. Taskaev, M. Bikchurina, T. Bykov, D. Kasatov, I. Kolesnikov, G. Ostreinov, S. Savinov, and E. Sokolova, Nucl. Instrum. Methods Phys. Res., Sect. B **554**, 165460 (2024). https://doi.org/10.1016/j.nimb.2024.165460
9. https://fgis.gost.ru/fundmetrology/registry/4/items/1414010.
10. A. V. Krasilnikov, N. B. Rodionov, A. P. Bolshakov, V. G. Ralchenko, S. K. Vartapetov, Y. E. Sizov, S. A. Meschaninov, A. G. Trapeznikov, V. P. Rodionova, V. N. Amosov, R. A. Khmelnitsky, and A. N. Kirichenko, Tech. Phys. **92**, 503 (2022). https://doi.org/10.21883/tp.2022.04.53607.226-21
11. D. Rigamonti, L. Giacomelli, G. Gorini, M. Nocente, M. Rebai, M. Tardocchi, M. Angelone, P. Batistoni, A. Cufar, Z. Ghani, S. Jednorog, A. Klix, E. Laszynska, S. Loreti, M. Pillon, S. Popovichev, N. Roberts, and D. Thomas, Meas. Sci. Technol. **29**, 045502 (2018). https://doi.org/10.1088/1361-6501/aaa675
12. A. V. Krasil'nikov and V. B. Kvaskov, *Natural Diamonds of Russia* (Polyaron, Moscow, 1997).
13. S. A. Kuvin, H. Y. Lee, B. Digiovine, A. Georgiadou, S. Mosby, D. Votaw, M. White, and L. Zavorka, Phys Rev. C **104**, 14603 (2021). https://doi.org/10.1103/physrevc.104.014603
14. D. Rigamonti, A. Dal Molin, A. Muraro, M. Rebai, L. Giacomelli, G. Gorini, M. Nocente, E. Perelli Cippo, S. Conroy, G. Ericsson, J. Eriksson, V. Kiptily, Z. Ghani, Ž. Štancar, and M. Tardocchi, Nucl. Fusion **64**, 016016 (2024). https://doi.org/10.1088/1741-4326/ad0a49
15. G. F. Knoll, *Radiation Detection and Measurement*, 4th ed. (Wiley, 2010).
16. Yu. M. Shirokov and N. P. Yudin, *Nuclear Physics* (Nauka, Moscow, 1980).
17. Two-body kinematics calculator and plotter. https://skisickness.com/2020/02/kinematics/.
18. O. V. Bochkarev, V. A. Vukolov, E. A. Koltydin, et al., Preprint Neutrons from the $^{7}\mathrm{Li}+\alpha$ Reaction in the Deuteron Energy Range 0.7–12.1 MeV (Kurchatovskii Institut, Moscow, 1994).
19. N. Dai, B. Qi, Ya. Mao, F. Zhuang, J. Yao, X. and Wang, Chin. J. Nucl. Phys. **9**, 103 (1987).
20. C. Nussbaum, Helvetica Phys. Acta **42**, 361 (1969). https://doi.org/10.5169/seals-114072
21. G. M. Osetinskii, B. Sikora, Ya. Tyke, and B. Fryshchin, *Study of reaction* ^{7}Li$(d,n)^{8}$Be (Dubna, Moscow oblast, 1970).
22. https://www-nds.iaea.org/exfor/ibandl.htm.
23. C. H. Johnson and C. C. Trail, Phys. Rev. **133**, B1183 (1964). https://doi.org/10.1103/physrev.133.b1183
24. Ch. Yan, H. Sun, X. Na, W. Ma, Yu. Cui, and X. Hu, Chin. J. Nucl. Phys. **2**, 137 (1980).
25. C. Milone and R. Potenza, Nuclear Physics **84**, 25 (1966). https://doi.org/10.1016/0029-5582(66)90430-5

26. J. Allison, K. Amako, J. Apostolakis, P. Arce, M. Asai, T. Aso, E. Bagli, A. Bagulya, S. Banerjee, G. Barrand, B. R. Beck, A. G. Bogdanov, D. Brandt, J. M. C. Brown, H. Burkhardt, P. H. Canal, D. Cano-Ott, S. Chauvie, K. Cho, G. A. P. Cirrone, G. Cooperman, M. A. Cortés-Giraldo, G. Cosmo, G. Cuttone, G. Depaola, L. Desorgher, X. Dong, A. Dotti, V. D. Elvira, G. Folger, Z. Francis, A. Galoyan, L. Garnier, M. Gayer, K. L. Genser, V. M. Grichine, S. Guatelli, P. Guèye, P. Gumplinger, A. S. Howard, I. Hřivnáčová, S. Hwang, S. Incerti, A. Ivanchenko, V. N. Ivanchenko, F. W. Jones, S. Y. Jun, P. Kaitaniemi, N. Karakatsanis, M. Karamitros, M. Kelsey, A. Kimura, T. Koi, H. Kurashige, A. Lechner, et al., Nucl. Instrum. Methods Phys. Res., Sect. A **835**, 186 (2016). https://doi.org/10.1016/j.nima.2016.06.125
27. S. A. Meshchaninov, N. B. Rodionov, A. V. Krasil'nikov, V. O. Saburov, E. I. Kazakov, A. A. Lychagin, S. R. Koryakin, Yu. A. Kashchuk, R. N. Rodionov, V. N. Amosov, and A. S. Dzhurik, Instrum. Exp. Tech. (2024).
28. J. Juna and K. Konecny, Rossendorf Reports 122, 195 (Zentralinstitut für Kernforschung, 1966).

AI tools may have been used in the translation or editing of this article.